Biomass Conversion and Biorefinery
https://doi.org/10.1007/s13399-024-05443-2

ORIGINAL ARTICLE

Ecofriendly synthesis of *Salmalia Malabarica gum* stabilized palladium nanoparticles: antibacterial and catalytic properties

Kondaiah Seku[1] · Babu Pejjai[2] · Ahmed I. Osman[3] · Syed Sulaiman Hussaini[1] · Mohammed Al Abri[4,5] · Nadavala Siva Kumar[6] · N. Satya Vijaya Kumar[7] · S. Shravan Kumar Reddy[8] · Kishor Kumar Sadasivuni[9] · Ahmed S. Al Fatesh[6] · Bhagavanth Reddy[10]

Received: 30 November 2023 / Revised: 3 February 2024 / Accepted: 14 February 2024

Abstract

Effluents containing dyes, discharged by various industries, have become a significant contributor to water pollution. This study explores the use of green-synthesized palladium nanoparticle (PdNP) catalysts, which offer enhanced catalytic performance compared to traditional methods. The research focuses on the synthesis of palladium nanoparticles using *Salmalia Malabarica* (SM) gum via a microwave-assisted process and investigates their catalytic and antibacterial properties. SEM analysis confirms the even distribution of PdNPs on the surface of SM gum. Furthermore, TEM analysis reveals a PdNPs size distribution of 10 ± 2 nm. XPS study was used to identify the chemical state of Pd in the synthesized nanoparticles. The results demonstrate that PdNPs are highly effective catalysts for the degradation of dyes such as Methylene Orange (MO), Rhodamine-B (Rh-B), and 4-Nitrophenol (4-NP), even after being reused five times. The catalytic activity of PdNPs was remarkable, achieved 99% dye degradation in four minutes. The degradation data of PdNPs on 4 -NP, MO and Rh-B dyes are followed by pseudo-first-order kinetics with 0.0087, 0.0152 and 0.0164 s^{-1}, respectively. Additionally, PdNPs exhibit exceptional antimicrobial activity against both bacterial and fungal strains. This synthesis process proves to be cost-effective, devoid of toxic chemicals, and remarkably rapid. The findings suggest promising applications for PdNPs in fields like nanomedicine and environmental remediation, reflecting their potential for addressing water pollution issues.

Keywords *Salmalia Malabarica* gum · Palladium nanoparticles · Methylene orange · Rhodamine-B · 4-Nitrophenol · Antimicrobial activity

✉ Kondaiah Seku
kondareddyseku@gmail.com; kondaiah.seku@utas.edu.om

✉ Ahmed I. Osman
aosmanahmed01@qub.ac.uk

✉ Bhagavanth Reddy
bhagavanth.g@gmail.com

[1] Department of Engineering, College of Engineering and Technology, University of Technology and Applied Sciences, Shinas, Sultanate of Oman

[2] Department of Physics, Sri Venkateshwara College of Engineering, Karakambadi Road, Tirupati 517507, India

[3] School of Chemistry and Chemical Engineering, Queen's University Belfast, Belfast, Northern Ireland BT9 5AG, UK

[4] Nanotechnology Research Center, Sultan Qaboos University, Muscat, Oman

[5] Department of Petroleum and Chemical Engineering, College of Engineering, Sultan Qaboos University, Muscat, Oman

[6] Department of Chemical Engineering, College of Engineering, King Saud University, P.O. Box 800, Riyadh 11421, Saudi Arabia

[7] Centre of excellence, Vignan's Foundation for Science, Technology & Research (Deemed to be University), Vadlamudi, Guntur, Andhra Pradesh 522213, India

[8] Department of Physics, Chaitanya Bharathi Institute of Technology, Gandipet, Hyderabad 500 075, India

[9] Centre for Advanced Materials, Qatar University, Doha, Qatar

[10] Department of Chemistry, Palamuru University PG center, Wanaparthi, India

Published online: 27 February 2024

1 Introduction

Effluents from industrial processes often carry a significant load of organic dyes, which can contain both organic and inorganic toxic compounds [1]; among these dyes commonly used in various industries, including Rhodamine -B, Methyl Orange, and Methyl Blue [2]. Furthermore, 4-Nitrophenol (4-NP) serves as a critical and versatile precursor in the production of agricultural chemicals, pharmaceutical drugs, and dyes. Notably, colorants and dyestuffs find extensive applications in sectors such as textiles and food production, further contributing to the release of nitrogen-containing organic compounds into the environment [3, 4]. The escalating use of these coloring agents and nitrogen-based organic substances stands out as a leading cause of water contamination, especially in surface water bodies. The pollutants discharged into the liquid phase pose a significant threat to aquatic ecosystems and their inhabitants. Exposure to these contaminants can result in various health issues, including but not limited to jaundice, cyanosis, quadriplegia, Heinz body formation, tissue necrosis, and more [5].

A significant challenge in dealing with dye pollutants is their large size, intricate molecular structure, high stability, and resistance to biodegradation. Due to their recalcitrance, these dyes must undergo treatment before being discharged into the environment. Conventionally, the treatment of wastewater containing such pollutants has relied on various techniques, including chemical treatments, electrochemical processes, ultrafiltration, coagulation, physisorption, chemical precipitation, and ion exchange methods [6]. In the quest for alternative methods to address this issue, researchers have explored the use of natural and synthetic adsorbents, such as animal charcoal, char/biochar, fibers derived from materials like coconut and jute, and graphene-oxide nanocomposites [7, 8]. Notably, graphene-oxide nanocomposites have shown promise in efficiently removing dyes from wastewater [9]. However, it's important to acknowledge that the aforementioned conventional methods have limitations. They often exhibit slow processing, high operational costs, and sometimes fall short in achieving complete removal of pollutants. Consequently, there is a pressing need for more efficient processes to effectively eliminate industrial effluents from the environment.

Currently, an efficient method for mitigating pollution in wastewater involves the utilization of nanocomposites or metal nanoparticles [10] in conjunction with $NaBH_4$. Numerous studies have explored the degradation of colored pollutants using various metal nanoparticles, including Cu, Au, and Ag [11–14], as well as metal oxide nanoparticles like TiO_2, ZnO, etc. [14–16]. Notably, PdNPs are renowned for their exceptional catalytic properties, which stem from their specific properties and chemical activity. PdNPs stand out as one of the most effective catalysts among metal nanoparticles. They have demonstrated their catalytic prowess in various processes, such as the reduction of nitroarenes and Suzuki coupling reactions [17]. These catalytic properties make PdNPs a valuable tool in the quest to combat water pollution, offering a rapid and effective means of eradicating pollutants from wastewater [18, 19].

Metal nanoparticles exhibit well-established antimicrobial applications. Many chronic diseases in humans started from bacterial and fungal infections, which are commonly treated with antibiotics due to their potent antimicrobial properties [20]. However, the excessive and inappropriate use of antibacterial agents has led to the development of antibiotic resistance, a growing global concern. Recent reports have raised the alarm about the emergence of super bacteria that may be impervious to all known antibiotics [21]. Bacterial resistance to antibiotics results in disease recurrence, posing a significant health challenge.

Inorganic nanoparticles, particularly metallic nanoparticles, have emerged as promising antibacterial agents to address these concerns [22]. Nanoparticles crafted from metals demonstrate remarkable efficacy in combating bacterial and microbial resistance and are well-suited for targeted drug delivery. Notably, PdNPs have come to the forefront in recent years, offering innovative solutions as antibacterial and antifungal agents [18, 23]. Their unique properties make them valuable contributors to the ongoing battle against antimicrobial resistance and infectious diseases.

PdNPs can be synthesized through various methods, including biological, chemical, sonochemical, electrochemical, or biochemical approaches [24, 25]. However, traditional chemical and physical methods have several drawbacks, such as the use of toxic chemicals that harm the environment and the need for costly, energy-intensive equipment operating at high temperatures and pressures. As a result of the use of harsh chemicals, chemical methods cause harm to the environment. These factors have prompted researchers worldwide to seek alternative, more cost-effective, environmentally friendly, and sustainable synthetic routes for PdNP production. Therefore, biological methods have been reported to synthesize NPs using biological materials such as plant extracts and biological species by researchers.

Biogenic synthesis offers a method to prepare nanoparticles using various plant and animal sources [26, 27]. Recent research has indicated that plant metabolites play a crucial role in capping and reducing agents during the green synthesis process [28]. A variety of leaf extracts and plant extracts were also used for the production of palladium nanoparticles, including *Solanum trilobatum* [28], *Anacardium occidentale* [29] and *pectin* versus *acaciagum*

as polysaccharides [30]. In this regard, we have developed a simple and green method for synthesising palladium nanoparticles from Na_2PdCl_4 by using a non-toxic, renewable natural plant extract of *Salmalia Malabarica* (SM) gum. SM gum is abundantly available in nature. Notably, SM gum boasts a wide range of medical applications, including its use in treating dysentery, diarrhea, menorrhagia, styptic, hemoptysis, influenza, pulmonary tuberculosis, enteritis, and more [31]. The gum comprises various compounds like terpenoids, glycosides, sugars, coloring agents, fatty compounds, and more. This study was undertaken to explore the promising applications of palladium nanoparticles in general and the potential medicinal properties of SM gum.

Herein, we present a rapid and straightforward approach for the synthesis of PdNPs using SM gum, employing the microwave (MW) technique. The MW synthesis method, known for its advantages over traditional approaches, is simple, scalable, environmentally friendly, unambiguous, and highly efficient. Notably, the MW method significantly reduces reaction time due to its intense energy supply and unique heating mode. Importantly, this study marks the first instance in the literature of biogenic PdNP synthesis using SM gum with the microwave irradiation method and explores their catalytic and antimicrobial applications. SM gum's stabilizing and reducing properties further enhance its effectiveness. Our research involves the synthesis of PdNPs with SM gum using microwave irradiation, followed by a comprehensive characterization by utilizing UV-Visible, FTIR, XRD, XPS, SEM, and TEM techniques. We also conducted reactions involving MO, Rh-B, along with 4-NP in the existence of $NaBH_4$, employing the synthesized PdNPs as a catalyst. Additionally, we studied the recyclability of the PdNPs and investigated their antibacterial activity against different bacterial strains.

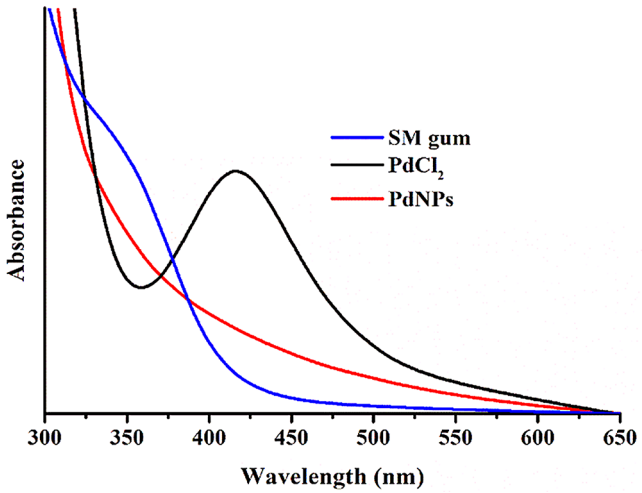

Fig. 1 UV- Vis absorption spectra of SM *gum*, Pd (II) solution, and PdNPs

2 Experimental information

2.1 Materials

Salmalia Malabarica (SM) gum was procured from Hyderabad, India. All chemicals, reagents, and materials of analytical grade used in this study were sourced from Sigma Aldrich and SD Fine-Chem Limited (Mumbai, India).

2.2 Preparation of SM gum extract

We mixed 0.5 g of finely powdered SM gum in 100 mL of double distilled (DD) water in a beaker as the reaction mixture was stirred continuously for 3 h at 60 ºC. Unreacted materials were removed by cooling the reaction mixture to room temperature and filtering it with a Whatman filter.

2.3 Biosynthesis of PdNPs with Salmalia Malabarica gum extract

The 18 mL of SM gum extract was mixed with 12 mL of 0.5 mM Na_2PdCl_4 solution in a beaker. 750 watts of microwave irradiation was applied to the reaction mixture for 7 min. The mixture was turned into a grey colour after microwave irradiation [32]. It suggests the palladium nanoparticles formation. After centrifuging for 10 min at 5000 rpm, the dark grey residue was obtained. We discarded the supernatant solution. PdNPs residue was washed three times with deionized water/methanol (1:1 v/v). These steps were used to remove unwanted substances from PdNPs. PdNPs were dried at 65 °C for 2 h. Furthermore, the obtained pure palladium nanoparticles were characterized and assessed for their biological and catalytic properties. The catalytic [32] and antibacterial activity procedure [33] and characterization techniques were present in the supplementary information file.

3 Results and discussion

3.1 UV-visible spectroscopic analysis

UV-Vis spectra were used to monitor the green synthesis of PdNPs using SM gum by a microwave irradiation method through a color evolution of the solution. A pale-yellow solution of Pd^{2+} ions changed to black when the SR gum was added. It indicates that PdNPs were formed by reducing Pd^{2+} to Pd^0. Figure 1 shows UV-Vis spectra of SR gum, Na_2PdCl_2 solution, and PdNPs. Absorption peaks were observed for Pd^{2+} ions at 360 and 450 nm [34], but no peak was detected for gum. A wavelength maximum was not observed for the PdNPs (gum + Pd^{2+}). The results

demonstrate that there are no Pd^{2+} ions in the solution, indicating that all Pd^{2+} ions have been reduced to Pd^{0}. UV-visible PdNPs do not exhibit plasmonic properties due to their non-absorbing properties [35].

3.2 FTIR spectroscopic analysis

The FTIR spectrum of green synthesized PdNPs using SM gum is shown in Fig. 2. The bands at 3395 cm^{-1} and 2912 cm^{-1} were associated with -OH and aliphatic -C-H bonds in the FTIR spectrum of SM gum (black line in Fig. 2). These two strong absorption bands observed at 1790 and 1690 cm^{-1} were attributed to C=O stretching in the spectrum of aliphatic ester and aromatic amide, respectively [36, 37]. The absorption bands found at 1508, 1302, and 1058 cm^{-1} were due to bending vibrations of N-H, C-O, and CO-O-CO for aromatic amides, aromatic esters, and anhydrides, respectively. The gum-capped PdNPs showed high-intensity vibrational bands (pink line in Fig. 2) at 3445, 2917, 1734, 1615, 1427, 1227, and 1041 cm^{-1}. Shifts in the bands were observed from 3395 to 3445, 2912 to 2917, 1790 to 1734, 1690 to 1615, 1508 to 1427, 1302 to 1227, and 1058 to 1041 cm^{-1} [38]. These results indicate that the synthesized PdNPs might be capped by functional groups present in the gum.

3.3 SEM and EDX analysis

The SEM analysis was conducted to assess the surface morphology and shape of the palladium nanoparticles. The results revealed that the PdNPs were predominantly quasi-spherical in shape. However, a few exhibited irregular shapes, as depicted in SEM images (Fig. 3a). Further examination indicated that the surface of the SM gum matrix

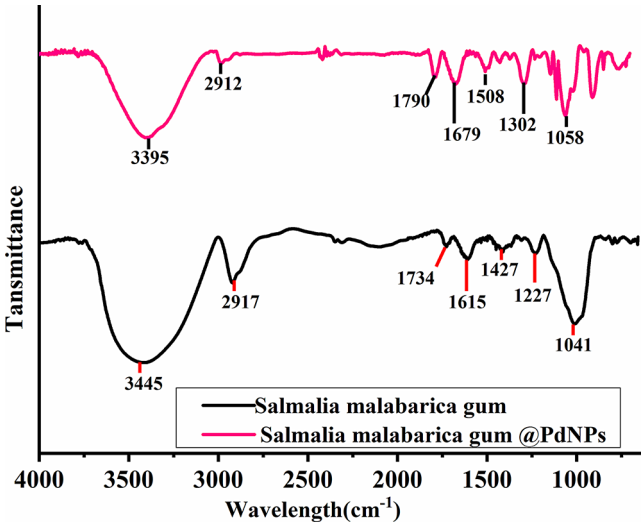

Fig. 2 FTIR spectra of (**a**) SM gum (black colour) and (**b**) PdNPs stabilized with SM gum (pink colour)

contained irregular and monodispersed palladium nanoparticles [39]. The energy-dispersive X-ray (EDX) spectrum displayed a distinct Palladium metal peak (Fig. 3b), providing unequivocal confirmation of the presence of palladium nanoparticles [40]. The EDX spectrum also suggested the successful immobilization of palladium nanoparticles on SM gum materials. This observation strongly indicates that palladium nanoparticles are uniformly distributed across the surface of the SM gum matrix.

3.4 XRD and TEM analyses

PdNPs were investigated by XRD to determine their crystallinity. XRD (Fig. 4) showed four characteristic peaks at 2θ = 39.65°, 45.24°, 65.14°, and 78.65°, respectively, and

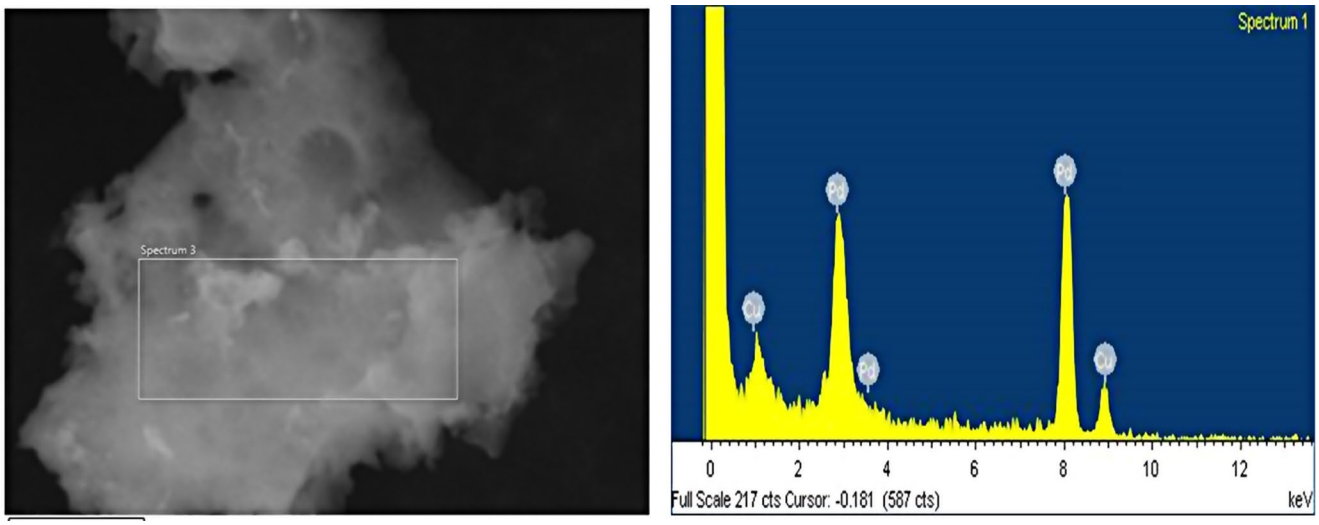

Fig. 3 SEM image of PdNPs stabilized with *SM* gum and its EDX spectrum

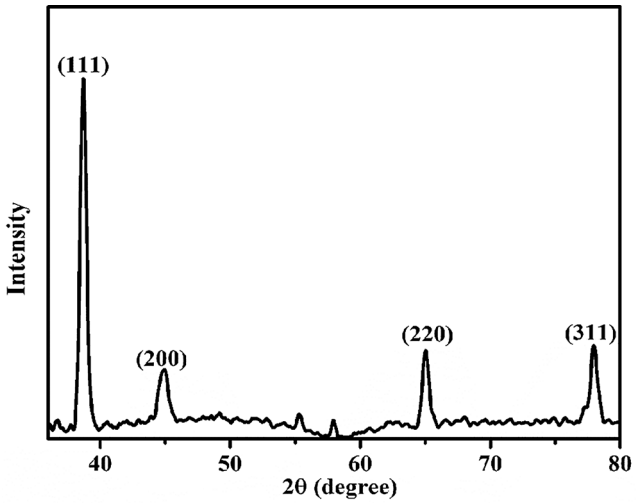

Fig. 4 Powder X-ray diffraction pattern of PdNPs

indexed to (111), (200), (222) and (311) planes of PdNPs (Joint Committee on Powder Diffraction Standards files No. 89–4897). XRD spectrum of the synthesized PdNPs showed that PdNPs were crystallized in a face-centered cubic structure [41]. The high intense peak (111) observed in the XRD pattern represents that PdNPs are more favoured to grow along the (111) orientation. Furthermore, the XRD pattern demonstrated the highly crystallized nature of the PdNPs. From Scherrer's equation $D = k\lambda/\beta\cos\theta$, an average crystallite size of 9.40 nm was found for PdNPs. In Scherrer's equation, λ represents the wavelength θ represents the Bragg angle; β represents the full width at half maximum of the strongest peak, and k is a shape-dependent Scherrer's constant [42]. The crystallite size of PdNPs calculated from XRD was in good agreement with the TEM analysis.

The TEM images (Fig. 5a) provide a clear depiction of the PdNPs that were synthesized, displaying their precise sizes and shapes. These particles were predominantly spherical in shape and uniform in size, with an average size of approximately 10 ± 2 nm. Furthermore, the PdNPs exhibited excellent dispersion, and high-resolution TEM images revealed a smooth surface [42]. As shown in Fig. 5b, there is a distinct spherical shape of 5 nm PdNPs. The TEM analysis clearly illustrates that the SM gum created a protective surface layer over the PdNPs, effectively preventing their aggregation. Moreover, the SEAD analysis (Fig. 5c) revealed well-defined lattice parameters, indicating that the synthesized PdNPs possess a high degree of crystallinity. A histogram developed from the analysis of 100 PdNPs is presented in Fig. 5d.

3.5 X-ray photoelectron spectroscopy (XPS) analysis

In order to determine the chemical state of Pd in nanoparticles, XPS was employed, which is a surface-sensitive analytical technique. The XPS spectra (Fig. 6) of Pd exhibited two distinct peaks: one at a high energy band of 340.98 eV and another at a lower energy of 335.97 eV. These peaks correspond to the Pd $3d_{3/2}$ and $3d_{5/2}$, respectively and fully

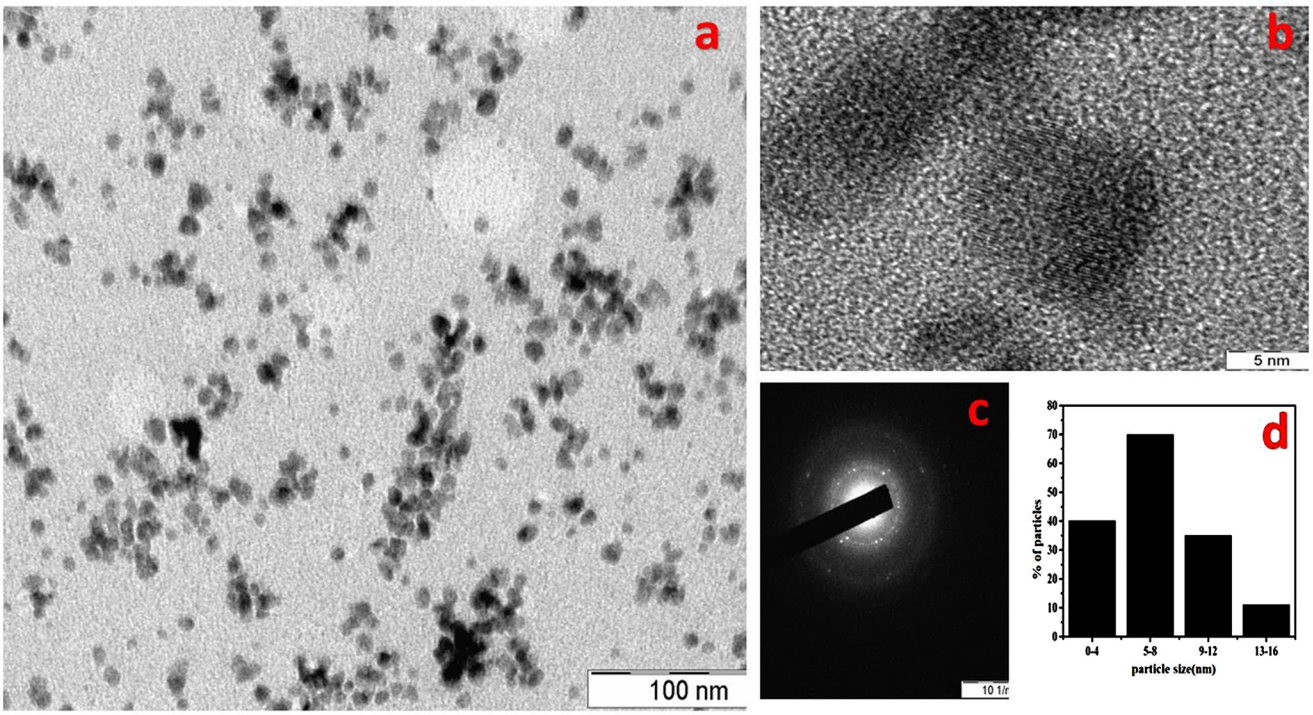

Fig. 5 (**a**) TEM image of PdNPs, (**b**) 5 nm of PdNPs, (**c**) SAED of PdNPs and (**d**) particle size distribution histogram

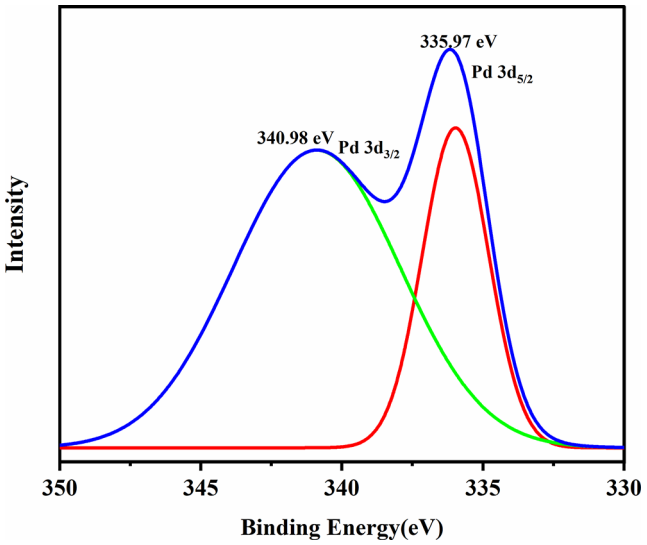

Fig. 6 XPS spectrum showing the binding energy of Pd 3d

match to reduced Pd(0)NPs. These findings are consistent with previous studies [43]. Therefore, the XPS spectrum analysis confirmed the successful preparation of zero-valent PdNPs using SM gum as a reducing and stabilizing agent [44].

3.6 Mechanism for PdNPs formation

SM gum played a dual role as both a reducing and stabilizing agent in the synthesis of PdNPs (as shown in Fig. 7), facilitating the reduction of Pd(II) to Pd(0). The composition of SM gum includes a variety of compounds such as terpenoids, carbohydrates, alcohols, esters, carboxylic acids, and carbonyl derivatives. Notably, the carboxylic, carbonyl, and hydroxyl groups within the gum were pivotal in reducing Pd (II) ions to their elemental Pd(0) state. Phytochemicals present in the gum possess potent antioxidant properties and high reducing capacity. This allowed them to effectively reduce Pd (II) ions to elemental palladium while undergoing oxidation themselves to form carbonyl and carboxyl groups [45]. Besides, the FTIR analysis corroborated the essential role of hydroxyl and carbonyl groups in both the synthesis and stabilization of PdNPs. The FTIR spectra obtained before and after PdNPs synthesis revealed a noticeable decrease in the hydroxyl and carbonyl bands [39]. At the same time, the COO- band at 1790 cm^{-1} was due to the groups on the surface of the nanoparticles. These results confirmed that the reduction and stabilization of PdNPs were mediated by the hydroxyl and carbonyl groups in SM gum [46].

3.7 Catalytic properties of PdNPs

Using 4-NP, MO, and Rh-B as substrates, PdNPs were evaluated for their catalytic activity. UV-Vis spectroscopy was used to monitor the reactions.

3.7.1 The catalytic reduction of 4-NP to 4-AP

A reduction of 4-NP to 4-AP in the presence of $NaBH_4$ was used to determine the catalytic effectiveness of PdNPs. Chemical reactions cause the colour to change from light yellow to deep yellow. The UV-Vis spectrum of 4-nitrophenol showed an absorption band at 315 nm [47]. Nitrophenolate ions are formed in solution when $NaBH_4$ is added to 4-NP, as indicated by the strong absorption peak at 405 nm (Fig. 8a). The peak intensity at 405 nm was retained for up to 120 min without the addition of PdNPs. This indicates that p-nitrophenolate was not reduced fully by $NaBH_4$ alone. By adding 5 mg of PdNPs to the reaction mixture (p-nitrophenolate ion), the catalytic effectiveness of PdNPs was tested and recorded over a variety of time intervals using a UV-Visible spectrophotometer [48]. Figure 8b reveals that the absorption peak intensity at 405 nm was decreased rapidly. There is an electron transfer process between PdNPs

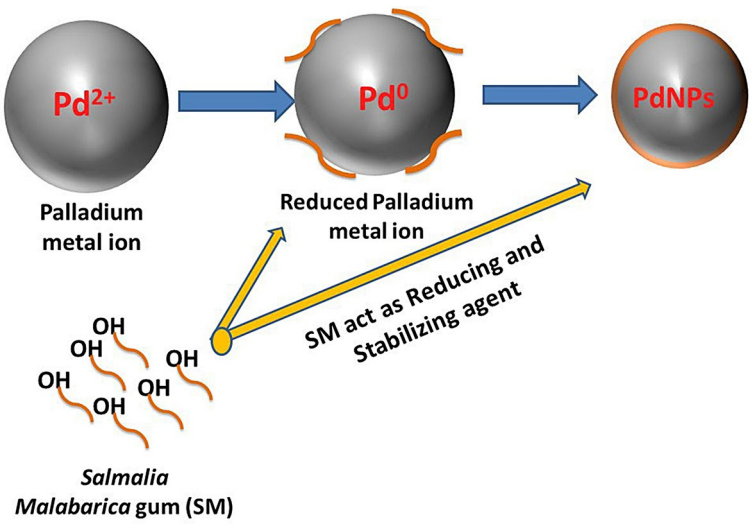

Fig. 7 Schematic representation of PdNPs formation mechanism

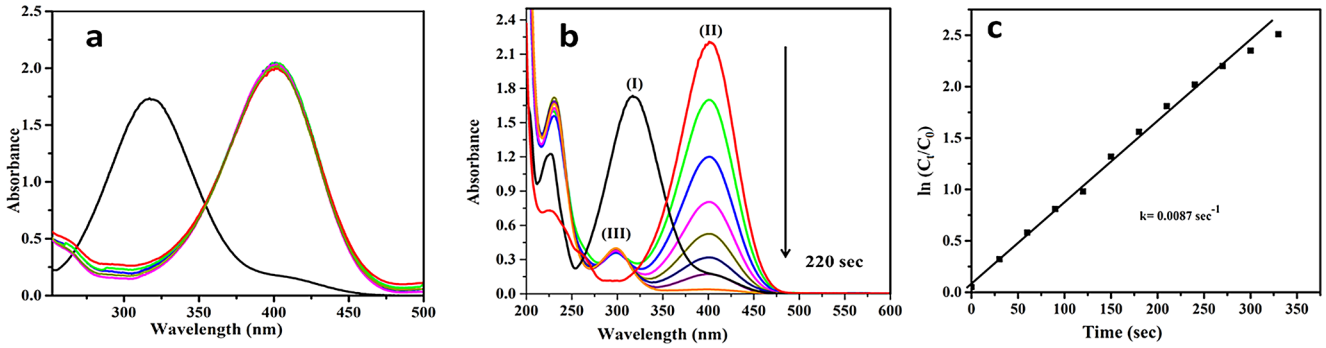

Fig. 8 (**a**) UV-Vis spectrum of 4-NP with $NaBH_4$ as the sole catalyst. (**b**) UV-Vis spectrum of 4-NP with a PdNPs catalyst in the presence of $NaBH_4$, showing the absorption maximum corresponding to (I) 4-NP, (II) 4-Nitrophenolate, and (III) 4-Aminophenol and (**c**) The reduction of 4-NP against ln (C_t/C_0) versus time

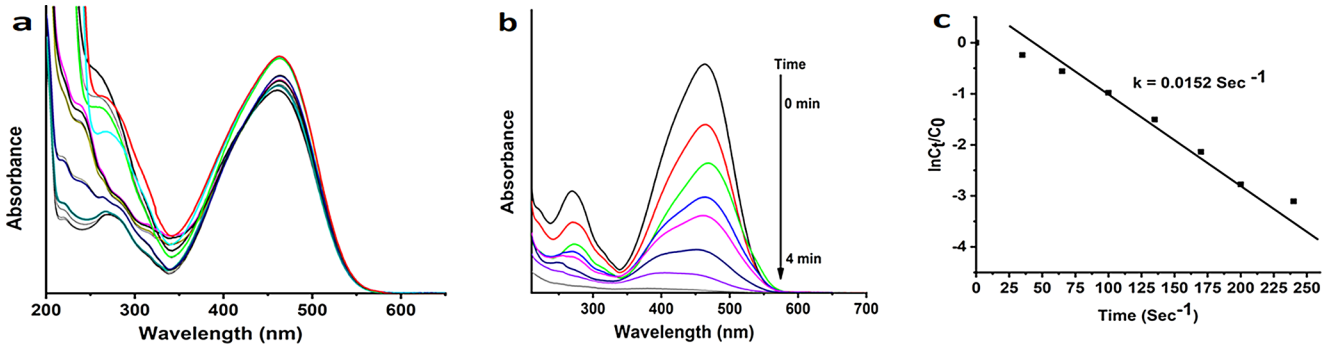

Fig. 9 UV -Visible Absorption spectra of (**a**) MO in the presence of $NaBH_4$ and in the absence of PdNPs, (**b**) Time-dependent MO reduction with $NaBH_4$ and PdNPs catalysts, and (**c**) Linear plot of (C_t/C_0) vs. time

and 4-nitrophenol [49]. After 220 s, we observed that the absorption peak at 405 nm gradually declined, and a new peak at 298 nm was developed, which implies the formation of 4-nitrophenol. 4-Nitrophenol was catalytically reduced in 220 s. As shown in Fig. 8c, ln (A_t/A_0) is plotted against reaction time. The plot indicates that the reaction followed a pseudo-first-order kinetic model, with a rate constant of 0.0087 s^{-1} at room temperature.

3.7.2 MO dye reduction studies

PdNPs catalytic efficacy was evaluated by reducing MO dye. Figure 9a shows the absorption spectrum of MO dye, which exhibits two distinct bands at 260 nm (n - π* electronic transition) and 450 nm (π - π* electronic transition). Figure 9a shows the absorption spectrum of MO dye when reduced with $NaBH_4$ without PdNPs. The two absorption bands remained unchanged even after 180 min without the PdNPs catalyst. It assumes that MO dye reduction was not completed [50, 51]. After adding 5 mg of PdNPs to the reaction mixture, the peak intensities (in Fig. 9b) were rapidly decreased. The dye solution was turned colourless from orange within 240 s, which indicates a complete reduction. A pseudo-first-order kinetic model is evident from Fig. 9c. A linear relationship was presented between ln C_t/C_0 and reaction time [52, 53]. The rate constant at the room temperature reaction was determined as 0.0152 s^{-1}.

3.7.3 Rhodamine-B dye reduction studies

Rh-B is used in textiles, paper, paints, leather, textile dyeing and other applications. Rh-B dye is highly soluble in water and has a basic nature. However, it can cause serious environmental and biological problems, perhaps irritate the eyes and skin and cause cancer. Utilizing PdNPs and $NaBH_4$ in conjunction with Rh-B dye, this study evaluated its catalytic degradation. In the presence of $NaBH_4$, Rh-B reduction shows absorption peaks at 615 and 665 nm in the UV-Vis spectrum [54, 55]. Even after 60 min, there was still a sharp peak at 550 nm in the case of Rh-B + $NaBH_4$ (Fig. 10a), suggesting that $NaBH_4$ alone could not be reduced by Rh-B effectively. PdNPs induced Rh-B reduction in 240 s (Fig. 10b). As the reaction time increased, the intensity of absorption bands at 550 nm decreased, accompanied by a change in colour from red to colourless [56, 57]. In the presence of PdNPs, Rh- Rh-B was reduced completely [58, 59]. Figure 10c showed a linear relationship between ln C_t/C_0 with reaction time, suggestive of pseudo-first-order kinetics

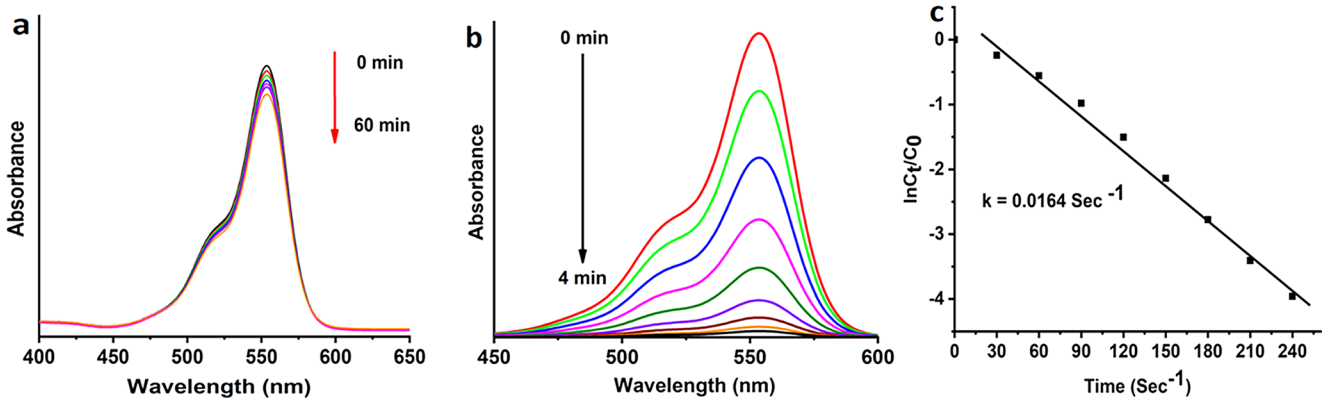

Fig. 10 UV -Visible Absorption spectra of (**a**) Rh-B in the presence of $NaBH_4$ and the absence of PdNPs, (**b**) Time-dependent Rh-B reduction with $NaBH_4$ and PdNPs catalysts, and (**c**) Linear plot of (C_t/C_0) vs. time

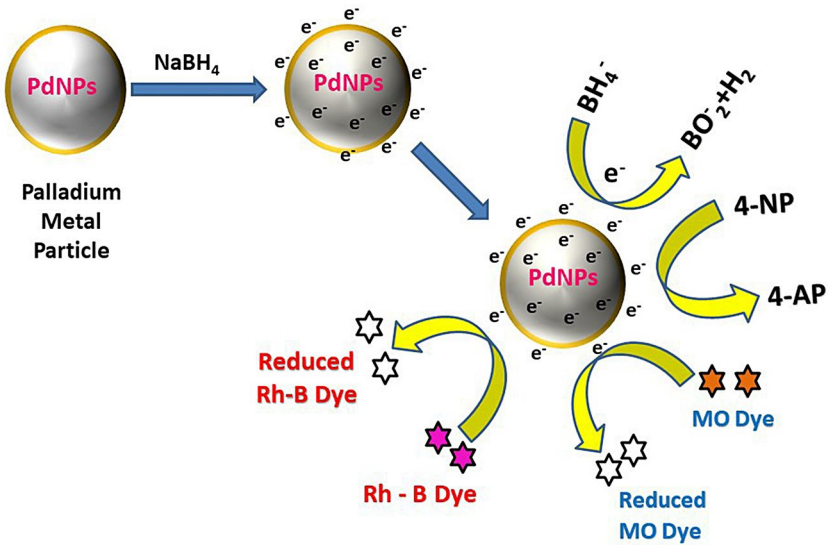

Fig. 11 Catalytic reduction mechanism of MO, Rh-B dyes, and 4-NP by PdNPs in the presence of $NaBH_4$.

at room temperature, with a constant rate of 0.0164 s^{-1}. The increased activity of PdNPs may be due to their higher surface-to-volume ratio, high surface coverage, enhanced electron transfer properties, and effective reduction of kinetic barriers [60, 61].

3.7.4 The catalytic reduction mechanism of the dyes

Figure 11 shows a possible catalytic reduction mechanism for 4-NP, Rh-B and MO, utilizing PdNPs as catalysts. Analytes' molecules (i.e., 4-NP, MO, and Rh-B) were absorbed on the surface of PdNPs during the first stage of the reduction process. PdNPs transferred electrons from BH^{4-} (donor) to analytes (acceptor) through electrostatic interactions [32]. These reactions have occurred at the surface of PdNPs [62]. By transferring electrons, dyes on the surface of PdNPs were reduced. As the PdNPs were desorbed from their surface, their byproducts diffused into the bulk of the solution.

3.7.5 Catalytic recyclability of PdNPs

PdNPs catalyst reusability was assessed by undergoing a variety of reduction cycles with 4-NP, MO, and Rh-B. Afterwards, the catalyst was washed, dried with methanol and water, and reused after being cleaned and dried [9, 63]. Figure 12 shows the recycling capability of PdNPs in the reduction reactions of 4-NP, MO, and Rh-B. After five cycles, PdNPs showed no significant loss in catalytic activity [64].

3.8 Antibacterial activity of PdNPs

Antibiotics employ several mechanisms to target bacteria, affecting critical processes like DNA replication, cell wall synthesis, and translation. However, despite these multifaceted attacks, bacteria have developed resistance mechanisms, rendering antibiotics ineffective. In contrast, the mode of action of metal nanoparticles, such as palladium nanoparticles, directly targeting the bacterial cell wall

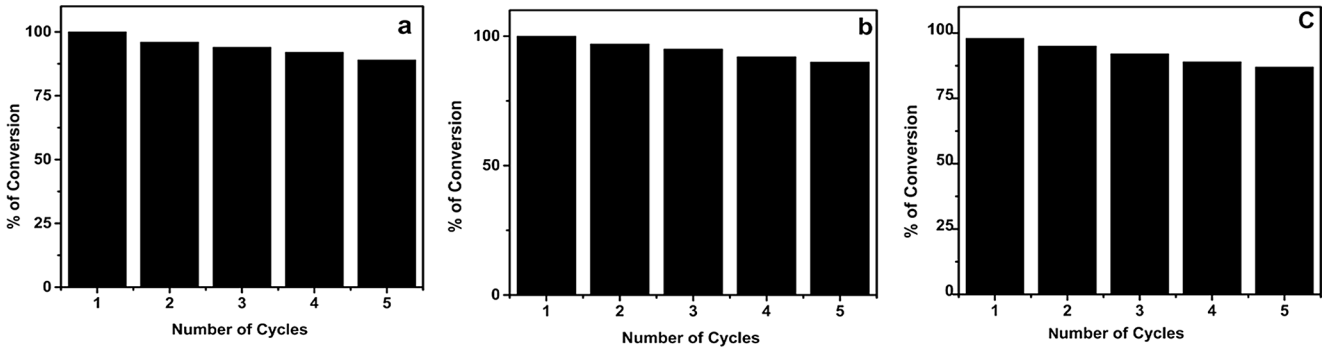

Fig. 12 Recyclability of PdNPs towards the reduction of (**a**) 4-NP, (**b**) MO, and (**c**) Rh-B dyes

Table 1 Antibacterial activity of PdNPs (Zone of inhibition in mm)

Microorganisms	Zone of Inhibition (mm) at different concentrations		
PdNPs concentrations	60 µg	80 µg	100 µg
Bacillus subtilis	15 ± 0.25	16 ± 0.22	19 ± 0.30
Bacillus cereus	12 ± 0.32	13 ± 0.27	15 ± 0.25
Escherichia coli	13 ± 0.41	14 ± 0.35	15 ± 0.27
Amoxicillin	16 ± 0.18	17 ± 0.20	19 ± 0.15

circumvents the issue of resistance compared to antibiotics [65]. Consequently, metal nanoparticles offer a promising alternative for combating microbes. Palladium nanoparticles, in particular, have garnered significant attention due to their unique biological properties, including their antimicrobial and anticancer capabilities [12]. These nanoparticles interact with bacteria in various ways. Smaller PdNPs can penetrate directly into bacterial cells, while larger nanoparticles remain outside the cells. This results in a continuous release of Pd^{2+} ions. These released ions disrupt the bacterial cell membrane by binding to it [66]. Once the cell wall is destabilized, palladium nanoparticles gain entry into the bacterial cell, where they interact with lipids, proteins, and DNA. This interaction leads to the dysfunction of the bacterial cell, ultimately inhibiting its growth and survival.

The PdNPs antibacterial tests were conducted against Gram-positive (*Bacillus subtilis* and *Bacillus cereus*) and Gram-negative (*Escherichia coli*). Disc diffusion was used to measure zone inhibitions of tested bacterial cultures [67, 68]. The zones of inhibition were observed with PdNPs (Table 1 & S. Figure 1). There were inhibition zones of 19 ± 0.30 mm and 15 ± 0.25 mm, respectively, for *Bacillus subtilis* and *Bacillus cereus* (Gram-positive strains). The inhibition zone for Gram-negative *Escherichia coli* was 15 ± 0.57 mm. Good antibacterial activity was demonstrated against *Bacillus subtilis* by PdNPs, but moderate activity was observed for other bacteria [69]. The antibacterial effect of PdNPs was significant for both Gram-positive and Gram-negative bacteria [64]. The antibacterial activity of PdNPs was increased by increasing its concentration. A comparison of the antibacterial activity of PdNPs is presented in Table 2.

Table 2 Comparison of the antibacterial efficacy of green synthesized PdNPs with extracts from various plants

Plant source	Zone of Inhibition (mm)			Reference
	Gram + Ve		Gram -Ve	
	B. subtilis	B. cereus	E. coli	
Filicium decipiens leaf extract	12 ± 0.25	-	27 ± 1.2	[70]
Melia azedarach leaf extract	8.3 ± 0.33		7.3 ± 0.33	[71]
lemon peel extract	12		13	[72]
Almond nuts extract	15 ± 0.03	12 ± 0.35	16 ± 0.3	[73]
Carica papaya aqueous leaf extract	15	-	11	[74]
Salmalia Malabarica gum	19 ± 0.30	15 ± 0.25	15 ± 0.27	Present work

4 Conclusions

This study focused on the eco-friendly and rapid synthesis of PdNPs using SM gum via microwave irradiation, presenting an efficient and environmentally benign method. The average particle size of PdNPs measured by XRD and TEM was 10 ± 2 nm with crystalline and spherical structures. The XPS spectra of PdNPs displayed two distinctive peaks at the high energy band 340.98 eV and low energy band 335.97 eV, which are the characteristics of Pd $3d_{3/2}$ and $3d_{5/2}$, respectively, and matches to fully reduced Pd (0) NPs. The catalytic activity of PdNPs was remarkable, achieving a 99% reduction of 4-NP, MO, and 98% reduction of Rh-B dyes. Significantly, the PdNPs catalyst could be reused multiple times without substantial loss of catalytic activity. Furthermore, these PdNPs exhibited strong antibacterial properties, with a zone of inhibition diameters measuring 19 ± 0.30, 15 ± 0.25 and 15 ± 0.27 mm for *Bacillus subtilis, Bacillus cereus* and *Escherichia coli*, respectively. *Bacillus subtilis* showed good antibacterial activity, while others showed moderate to good antibacterial activity. This study underscores the potential of PdNPs to swiftly reduce environmental pollutants and suggests their suitability for future biomedical applications.

Supplementary Information The online version contains supplementary material available at https://doi.org/10.1007/s13399-024-05443-2.

Acknowledgements Dr. Kondaiah Seku is thankful to The Research Council, Sultanate of Oman, for the financial support from the TRC Research Grant (TRC proposal grant No: BFP/RGP/EI/21/229). The KSU authors would like to extend their sincere appreciation to the Researchers Supporting Project number (RSP2024R368), King Saud University, Riyadh, Saudi Arabia.

Author contributions Kondaiah Seku: Conceptualization, Investigation, Writing -Original Draft, Funding Acquisition; Babu Pejjai: Data curation and Characterization works analysis; Ahmed I. Osman: Visualization, and Data Curation; Syed Sulaiman Hussaini: Data curation and Visualization; Mohammed Al-Abri: Characterization works, Data analysis and Data validation; Nadavala Siva Kumar: Data Curation and Formal Analysis; N. Satya Vijaya Kumar: Characterization works and data analysis; S. Shravan Kumar Reddy: Data analysis and data curation; Kishor Kumar Sadasivuni: Data analysis and Data validation; Ahmed S. Al Fatesh: Data curation and Visualization; Bhagavanth Reddy G: Supervision, Investigation, Data curation, Review the Original draft and Experimental.

Data availability Data will be made available upon reasonable request.

Declarations

Ethics approval and consent to participate Does not require any ethical approval since we could not use any animals or Humans for this study.

Conflict of interest The authors declare that they do not have any conflict of interest.

References

1. Waring DR, Hallas G, Gregory P (2013) The Chemistry and Application of Dyes Plenum Press • New York and London 2 Classification of Dyes by Chemical Structure, 17–47
2. Osman AI, El-Monaem EMA, Elgarahy AM, Aniagor CO, Hosny M, Farghali M, Rashad E, Ejimofor MI, López-Maldonado EA, Ihara I, Yap PS, Rooney DW, Eltaweil AS (2023) Methods to prepare biosorbents and magnetic sorbents for water treatment: a review. Springer International Publishing. https://doi.org/10.1007/s10311-023-01603-4
3. Ismail GA, Sakai H (2022) Review on effect of different type of dyes on advanced oxidation processes (AOPs) for textile color removal. Chemosphere 291:311–320. https://doi.org/10.1016/j.chemosphere.2021.132906
4. Fleischmann C, Lievenbrück M, Ritter H (2015) Polymers and dyes: developments and applications. Polym (Basel) 7:717–746. https://doi.org/10.3390/polym7040717
5. Lellis B, Fávaro-Polonio CZ, Pamphile JA, Polonio JC (2019) Effects of textile dyes on health and the environment and bioremediation potential of living organisms. Biotechnol Res Innov 3:275–290. https://doi.org/10.1016/j.biori.2019.09.001
6. Varjani S, Rakholiya P, Shindhal T, Shah AV, Ngo HH (2021) Trends in dye industry effluent treatment and recovery of value added products. J Water Process Eng 39:101734. https://doi.org/10.1016/j.jwpe.2020.101734
7. Osman AI, Elgarahy AM, Mehta N, Al-Muhtaseb AH, Al-Fatesh AS, Rooney DW (2022) ACS Sustain Chem Eng 10:12433–12447. https://doi.org/10.1021/acssuschemeng.2c04095. Facile Synthesis and Life Cycle Assessment of Highly Active Magnetic Sorbent Composite Derived from Mixed Plastic and Biomass Waste for Water Remediation
8. Khatri A, Peerzada MH, Mohsin M, White M (2015) A review on developments in dyeing cotton fabrics with reactive dyes for reducing effluent pollution. J Clean Prod 87:50–57. https://doi.org/10.1016/j.jclepro.2014.09.017
9. Obayomi KS, Lau SY, Danquah MK, Zhang J, Chiong T, Meunier L, Gray SR, Rahman MM (2023) Green synthesis of graphene-oxide based nanocomposites for efficient removal of methylene blue dye from wastewater. Desalination 564:116749. https://doi.org/10.1016/j.desal.2023.116749
10. Verma N, Chundawat TS, Chandra H, Vaya D (2023) An efficient time reductive photocatalytic degradation of carcinogenic dyes by TiO2-GO nanocomposite. Mater Res Bull 158:112043. https://doi.org/10.1016/j.materresbull.2022.112043
11. Seku K, Gangapuram BR, Pejjai B, Hussain M, Hussaini SS, Golla N, Kadimpati KK (2019) Eco-friendly synthesis of gold nanoparticles using carboxymethylated gum Cochlospermum gossypium (CMGK) and their catalytic and antibacterial applications. Chem Pap 73. https://doi.org/10.1007/s11696-019-00722-z
12. Seku K, Hussaini SS, Hussain M, Siddiqui MA, Golla N, Ravinder D, Reddy B (2022) Synthesis of Frankincense gum stabilized AgNPs by microwave irradiation and their catalytic, antioxidant, and antibacterial properties. Phys E Low-Dimensional Syst Nanostruct 140:115169. https://doi.org/10.1016/j.physe.2022.115169
13. Pant B, Pant HR, Barakat NAM, Park M, Jeon K, Choi Y, Kim HY (2013) Carbon nanofibers decorated with binary semiconductor (TiO2/ZnO) nanocomposites for the effective removal of organic pollutants and the enhancement of antibacterial activities. Ceram Int 39:7029–7035. https://doi.org/10.1016/j.ceramint.2013.02.041
14. Iuliano M, Ponticorvo E, Cirillo C, Adami R, Sarno M (2023) Catalytic hydrogenation of organic dyes by ag and au magnetic nanoparticles supported on nanocellulose from waste pistachio shells. Mol Catal 544:113179. https://doi.org/10.1016/j.mcat.2023.113179
15. Bel Hadjltaief H, Ben Ameur S, Da Costa P, Ben Zina M, Elena M, Galvez (2018) Photocatalytic decolorization of cationic and anionic dyes over ZnO nanoparticle immobilized on natural Tunisian clay. Appl Clay Sci 152:148–157. https://doi.org/10.1016/j.clay.2017.11.008
16. Han L, Su B, Liu G, Ma Z, An X (2018) Synthesis of oxygen vacancy-rich black TiO2 nanoparticles and the visible light photocatalytic performance. Mol Catal 456:96–101. https://doi.org/10.1016/j.mcat.2018.07.006
17. Baran NY, Baran T, Nasrollahzadeh M, Varma RS (2019) Pd nanoparticles stabilized on the Schiff base-modified boehmite: Catalytic role in Suzuki coupling reaction and reduction of

nitroarenes. J Organomet Chem 900. https://doi.org/10.1016/j.jorganchem.2019.120916
18. Thirumalraj B, Rajkumar C, Chen S-M, Veerakumar P, Perumal P, Liu S-B (2018) Carbon aerogel supported palladium-ruthenium nanoparticles for electrochemical sensing and catalytic reduction of food dye. Sens Actuators B Chem 257:48–59. https://doi.org/10.1016/j.snb.2017.10.112
19. V PP, Sathe PRV, Mahalingam U (2019) Graphene boosted silver nanoparticles as surface enhanced Raman spectroscopic sensors and photocatalysts for removal of standard and industrial dye contaminants. Sens Actuators B Chem 281:679–688. https://doi.org/10.1016/j.snb.2018.11.007
20. Nemeth J, Oesch G, Kuster SP (2015) Bacteriostatic versus bactericidal antibiotics for patients with serious bacterial infections: systematic review and meta-analysis. J Antimicrob Chemother 70:382–395. https://doi.org/10.1093/jac/dku379
21. Cesa A, Arias BE, Murray (2018) Antibiotic-resistant bugs in the 21st Century — a clinical Super-challenge. N Engl J Med 360:439–443
22. Dizaj SM, Lotfipour F, Barzegar-Jalali M, Zarrintan MH, Adibkia K (2014) Antimicrobial activity of the metals and metal oxide nanoparticles. Mater Sci Eng C 44:278–284. https://doi.org/10.1016/j.msec.2014.08.031
23. Kasinathan K, Marimuthu K, Murugesan B, Samayanan S, Cai Y, Rathinam C (2021) Facile synthesis of highly biologically active chitosan functionalized 2D WS2 nanocomposite anchored with palladium nanoparticles for antibacterial and anticancer activity: In-vitro biomedical evaluation. J Mol Liq 335:116582. https://doi.org/10.1016/j.molliq.2021.116582
24. Rüllmann M, Gabriel C, Alteheld A, Schütte M, Duwenhorst J, Prissok F, Egbers G (2006) Compact and Foamed Magnetorheological Polyurethanes, 2–3
25. Prasad SR, Padvi MN, Suryawanshi SS, Shaikh YI, Chaudhary LS, Samant AP, Prasad NR (2020) Bio-inspired synthesis of catalytically and biologically active palladium nanoparticles using Bos taurus urine. SN Appl Sci 2. https://doi.org/10.1007/s42452-020-2382-3
26. Sengan M, Veeramuthu D, Veerappan A (2018) Photosynthesis of silver nanoparticles using Durio zibethinus aqueous extract and its application in catalytic reduction of nitroaromatics, degradation of hazardous dyes and selective colorimetric sensing of mercury ions. Mater Res Bull 100:386–393. https://doi.org/10.1016/j.materresbull.2017.12.038
27. Nasrollahzadeh M, Sajjadi M, Maham M, Sajadi SM, Barzinjy AA (2018) Biosynthesis of the palladium/sodium borosilicate nanocomposite using Euphorbia milii extract and evaluation of its catalytic activity in the reduction of chromium(VI), nitro compounds and organic dyes. Mater Res Bull 102:24–35. https://doi.org/10.1016/j.materresbull.2018.01.032
28. Kanchana A, Devarajan S, Ayyappan SR (2010) Green synthesis and characterization of palladium nanoparticles and its conjugates from solanum trilobatum leaf extract. Nano-Micro Lett 2:169–176. https://doi.org/10.5101/nml.v2i3.p169-176
29. Sheny DS, Philip D, Mathew J (2012) Rapid green synthesis of palladium nanoparticles using the dried leaf of Anacardium occidentale, Spectrochim. Acta - Part A Mol. Biomol Spectrosc 91:35–38. https://doi.org/10.1016/j.saa.2012.01.063
30. Emam HE, Saad NM, Abdallah AEM, Ahmed HB (2020) Acacia gum versus pectin in fabrication of catalytically active palladium nanoparticles for dye discoloration. Int J Biol Macromol 156:829–840. https://doi.org/10.1016/j.ijbiomac.2020.04.018
31. De D, Ali KM, Chatterjee K, Bera TK, Ghosh D (2012) Antihyperglycemic and antihyperlipidemic effects of n-hexane fraction from the hydro-methanolic extract of sepals of Salmalia malabarica in Streptozotocin-induced diabetic rats. J Complement Integr Med 9. https://doi.org/10.1515/1553-3840.1565
32. Seku K, Sulaiman Hussaini S, Golla N, Mangatayaru G, D KSMV, Rapolu S, Bandi R, Reddy B (2020) Microwave-assisted synthesis of palladium nanoparticles using Frankincense resin and evaluation of their catalytic properties. Mater Lett 278. https://doi.org/10.1016/j.matlet.2020.128427
33. Sree GS, Mohan BS, Reddy BJM, Ranjitha KVB (2021) Deterioration of Cadmium and pathogens from contaminated water using hydrothermally prepared NiO-ZnO-RGO composite. J Mater Res Technol 10:976–987. https://doi.org/10.1016/j.jmrt.2020.12.065
34. Gnanasekar S, Murugaraj J, Dhivyabharathi B, Krishnamoorthy V, Jha PK, Seetharaman P, Vilwanathan R, Sivaperumal S (2018) Antibacterial and cytotoxicity effects of biogenic palladium nanoparticles synthesized using fruit extract of Couroupita guianensis Aubl. J Appl Biomed 16:59–65. https://doi.org/10.1016/j.jab.2017.10.001
35. Nguyen TD, Vo TT, Nguyen CH, Doan VD, Dang CH (2019) Biogenic palladium nanoclusters supported on hybrid nanocomposite 2-hydroxypropyl-β-cyclodextrin/alginate as a recyclable catalyst in aqueous medium. J Mol Liq 276:927–935. https://doi.org/10.1016/j.molliq.2018.12.138
36. Li G, Li Y, Wang Z, Liu H (2017) Green synthesis of palladium nanoparticles with carboxymethyl cellulose for degradation of azo-dyes. Mater Chem Phys 187:133–140. https://doi.org/10.1016/j.matchemphys.2016.11.057
37. Guo Y, Cao F, Li Y (2018) Solid phase synthesis of nitrogen and phosphor co-doped carbon quantum dots for sensing Fe3 + and the enhanced photocatalytic degradation of dyes. Sens Actuators B Chem 255:1105–1111. https://doi.org/10.1016/j.snb.2017.08.104
38. Khan ZUH, Shah NS, Iqbal J, Khan AU, Imran M, Alshehri SM, Muhammad N, Sayed M, Ahmad N, Kousar A, Ashfaq M, Howari F, Tahir K (2020) Biomedical and photocatalytic applications of biosynthesized silver nanoparticles: Ecotoxicology study of brilliant green dye and its mechanistic degradation pathways. J Mol Liq 319:114114. https://doi.org/10.1016/j.molliq.2020.114114
39. Anjum F, Gul S, Khan MI, Khan MA (2020) Efficient synthesis of palladium nanoparticles using guar gum as stabilizer and their applications as catalyst in reduction reactions and degradation of azo dyes. Green Process Synth 9:63–76. https://doi.org/10.1515/gps-2020-0008
40. Zhu J, Zhang X, Qin Z, Zhang L, Ye Y, Cao M, Gao L, Jiao T (2021) Preparation of PdNPs doped Chitosan-based composite hydrogels as highly efficient catalysts for reduction of 4-nitrophenol, colloids surfaces a physicochem. Eng Asp 611:125889. https://doi.org/10.1016/j.colsurfa.2020.125889
41. Fathima JB, Pugazhendhi A, Oves M, Venis R (2018) Synthesis of eco-friendly copper nanoparticles for augmentation of catalytic degradation of organic dyes. J Mol Liq 260:1–8. https://doi.org/10.1016/j.molliq.2018.03.033
42. Kora AJ, Rastogi L (2016) Catalytic degradation of anthropogenic dye pollutants using palladium nanoparticles synthesized by gum olibanum, a glucuronoarabinogalactan biopolymer, Ind. Crops Prod. 81(1) Kora 1–10. https://doi.org/10.1016/j.indcrop.2015.11.055
43. Dadigala R, Bandi R, Alle M, Park C-W, Han S-Y, Kwon G-J, Lee S-H (2022) Effective fabrication of cellulose nanofibrils supported pd nanoparticles as a novel nanozyme with peroxidase and oxidase-like activities for efficient dye degradation. J Hazard Mater 436:129165. https://doi.org/10.1016/j.jhazmat.2022.129165
44. Ivandini TA, Luhur MSP, Khalil M, Einaga Y (2021) Modification of boron-doped diamond electrodes with gold-palladium nanoparticles for an oxygen sensor. Analyst 146:2842–2850. https://doi.org/10.1039/d0an02414g
45. Vijilvani C, Bindhu MR, Frincy FC, AlSalhi MS, Sabitha S, Saravanakumar K, Devanesan S, Umadevi M, Aljaafreh MJ, Atif M (2020) Antimicrobial and catalytic activities of biosynthesized gold, silver and palladium nanoparticles from Solanum Nigurum

leaves. J Photochem Photobiol B Biol 202:111713. https://doi.org/10.1016/j.jphotobiol.2019.111713
46. Man RWY, Brown ARC, Wolf MO (2012) Mechanism of formation of Palladium nanoparticles: Lewis Base assisted, Low-Temperature Preparation of Monodisperse Nanoparticles. Angew Chemie 124:11512–11515. https://doi.org/10.1002/ange.201205057
47. Seku K, Gangapuram BR, Pejjai B, Kadimpati KK, Golla N (2018) Microwave-assisted synthesis of silver nanoparticles and their application in catalytic, antibacterial and antioxidant activities. J Nanostructure Chem 8:179–188. https://doi.org/10.1007/s40097-018-0264-7
48. Saravanakumar K, Priya VS, Balakumar V, Prabavathi SL, Muthuraj V (2022) Noble metal nanoparticles (Mx = ag, au, pd) decorated graphitic carbon nitride nanosheets for ultrafast catalytic reduction of anthropogenic pollutant, 4-nitrophenol. Environ Res 212:113185. https://doi.org/10.1016/J.ENVRES.2022.113185
49. Gerelbaatar K, Tsogoo A, Dashzeveg R, Tsedev N, Ganbold EO (2018) Reduction of 2,4-dinitrophenol to 2,4-diaminophenol using AuNPs and AgNPs as catalyst. Solid State Phenom 271 SSP 76–84. https://doi.org/10.4028/www.scientific.net/SSP.271.76
50. Ismail M, Gul S, Khan MI, Khan MA, Asiri AM, Khan SB (2019) Medicago polymorpha-mediated antibacterial silver nanoparticles in the reduction of methyl orange. Green Process Synth 8:118–127. https://doi.org/10.1515/gps-2018-0030
51. Mohammadi P, Daneshafruz H, Sheibani H (2021) Gold nanoparticles on cyanuric citric acid functionalized magnetic SBA-16 as an effective catalyst for dye reduction. Phys E Low-Dimensional Syst Nanostruct. https://doi.org/10.1016/j.physe.2020.114392
52. Khezami L, Ben Aissa MA, Modwi A, Guesmi A, Algethami FK, Bououdina M (2022) Efficient removal of organic dyes by Cr-doped ZnO nanoparticles. Biomass Convers Biorefinery. https://doi.org/10.1007/s13399-022-02952-w
53. Islam MT, Jing H, Yang T, Zubia E, Goos AG, Bernal RA, Botez CE, Narayan M, Chan CK, Noveron JC (2018) Fullerene stabilized gold nanoparticles supported on titanium dioxide for enhanced photocatalytic degradation of methyl orange and catalytic reduction of 4-nitrophenol. J Environ Chem Eng 6:3827–3836. https://doi.org/10.1016/j.jece.2018.05.032
54. Ogoko EC, Kelle HI, Akintola O, Eddy NO (2023) Experimental and theoretical investigation of Crassostrea gigas (gigas) shells based CaO nanoparticles as a photocatalyst for the degradation of bromocresol green dye (BCGD) in an aqueous solution. Biomass Convers Biorefinery. https://doi.org/10.1007/s13399-023-03742-8
55. Muraro PCL, Mortari SR, Vizzotto BS, Chuy G, dos Santos C, Brum LFW, da Silva WL (2020) Iron oxide nanocatalyst with titanium and silver nanoparticles: synthesis, characterization and photocatalytic activity on the degradation of rhodamine B dye. Sci Rep 10:1–9. https://doi.org/10.1038/s41598-020-59987-0
56. Kumar S, Sharma SK, Kaushik RD, Purohit LP (2021) Chalcogen-doped zinc oxide nanoparticles for photocatalytic degradation of rhodamine B under the irradiation of ultraviolet light. Mater Today Chem 20:100464. https://doi.org/10.1016/j.mtchem.2021.100464
57. Chandhru M, Rani SK, Vasimalai N (2020) Reductive degradation of toxic six dyes in industrial wastewater using diaminobenzoic acid capped silver nanoparticles. J Environ Chem Eng 8:104225. https://doi.org/10.1016/j.jece.2020.104225
58. Meneceur S, Hemmami H, Bouafia A, Laouini SE, Tedjani ML, Berra D, Mahboub MS (2022) Photocatalytic activity of iron oxide nanoparticles synthesized by different plant extracts for the degradation of diazo dyes Evans blue and Congo red, Biomass Convers. Biorefinery. https://doi.org/10.1007/s13399-022-02734-4
59. Yadav AA, Kang SW, Hunge YM (2021) Photocatalytic degradation of rhodamine B using graphitic carbon nitride photocatalyst. J Mater Sci Mater Electron 32:15577–15585. https://doi.org/10.1007/s10854-021-06106-y
60. Sharmila G, Haries S, Farzana Fathima M, Geetha S, Manoj Kumar N, Muthukumaran C (2017) Enhanced catalytic and antibacterial activities of phytosynthesized palladium nanoparticles using Santalum album leaf extract. Powder Technol 320:22–26. https://doi.org/10.1016/j.powtec.2017.07.026
61. Ag C, Chains GO, Riecken JF, Heymann G, Behrmann N, Johrendt D, Rayaprol S, Pöttgen R, Huppertz H (n.d) High–Pressure Intermetallic Germanide Oxide https://doi.org/10.1002/anie.200123456
62. Malik MA, Alshehri AA, Abomuti MA, Danish EY, Patel R (2021) Bioengineered matricaria recutita extract-assisted palladium nanoparticles for the Congo red dye degradation and catalytic reduction of 4-nitrophenol to 4-aminophenol, Toxics. 9. https://doi.org/10.3390/toxics9050103
63. Wang N, Hu Y, Zhang Z (2017) Sustainable catalytic properties of silver nanoparticles supported montmorillonite for highly efficient recyclable reduction of methylene blue. Appl Clay Sci 150:47–55. https://doi.org/10.1016/j.clay.2017.08.024
64. Sharmila G, Haries S, Farzana Fathima M, Geetha S, Manoj Kumar N, Muthukumaran C (2017) Enhanced catalytic and antibacterial activities of phytosynthesized palladium nanoparticles using Santalum album leaf extract. Powder Technol 320:22–26. https://doi.org/10.1016/j.powtec.2017.07.026
65. Das P, Dutta T, Manna S, Loganathan S, Basak P (2022) Facile green synthesis of non-genotoxic, non-hemolytic organometallic silver nanoparticles using extract of crushed, wasted, and spent Humulus lupulus (hops): Characterization, anti-bacterial, and anti-cancer studies. Environ Res 204:111962. https://doi.org/10.1016/J.ENVRES.2021.111962
66. Seku K, Hussaini SS, Pejjai B, Al Balushi MMS, Dasari R, Golla N, Reddy GB (2020) A rapid microwave-assisted synthesis of silver nanoparticles using Ziziphus jujuba Mill fruit extract and their catalytic and antimicrobial properties. Chem Pap 1–14. https://doi.org/10.1007/s11696-020-01386-w
67. Anand K, Tiloke C, Phulukdaree A, Ranjan B, Chuturgoon A, Singh S, Gengan RM (2016) Biosynthesis of palladium nanoparticles by using Moringa oleifera flower extract and their catalytic and biological properties. J Photochem Photobiol B Biol 165:87–95. https://doi.org/10.1016/j.jphotobiol.2016.09.039
68. Bisht NS, Tripathi AH, Pant M, Kumar Upadhyay S, Sahoo NG, Mehta SPS, Dandapat A (2022) A facile synthesis of palladium nanoparticles decorated bismuth oxybromide nanostructures with exceptional photo-antimicrobial activities. Colloids Surf B Biointerfaces 217:112640. https://doi.org/10.1016/j.colsurfb.2022.112640
69. Chen Y, Chen Z, Yang D, Zhu L, Liang Z, Pang Y, Zhou L (2022) Novel Microbial Palladium nanoparticles with a high Photothermal Effect for Antibacterial Applications, ACS Omega. https://doi.org/10.1021/acsomega.2c07037
70. Sharmila G, Farzana Fathima M, Haries S, Geetha S, Manoj Kumar N, Muthukumaran C (2017) Green synthesis, characterization and antibacterial efficacy of palladium nanoparticles synthesized using Filicium decipiens leaf extract. J Mol Struct 1138:35–40. https://doi.org/10.1016/j.molstruc.2017.02.097
71. Bhakyaraj K, Kumaraguru S, Gopinath K, Sabitha V, Kaleeswarran PR, Karthika V, Sudha A, Muthukumaran U, Jayakumar K, Mohan S, Arumugam A (2017) Eco-friendly synthesis of Palladium nanoparticles using Melia azedarach Leaf Extract and their evaluation for Antimicrobial and Larvicidal activities. J Clust Sci 28:463–476. https://doi.org/10.1007/s10876-016-1114-8
72. Liang Y, Demir H, Wu Y, Aygun A, Elhouda Tiri RN, Gur T, Yuan Y, Xia C, Demir C, Sen F, Vasseghian Y (2022) Facile synthesis of biogenic palladium nanoparticles using biomass strategy and application as photocatalyst degradation for textile dye

pollutants and their in-vitro antimicrobial activity. Chemosphere 306:135518. https://doi.org/10.1016/j.chemosphere.2022.135518

73. Sadalage PS, Pawar KD (2023) Adsorption and removal of ethidium bromide from aqueous solution using optimized biogenic catalytically active antibacterial palladium nanoparticles. Environ Sci Pollut Res 30:5005–5026. https://doi.org/10.1007/s11356-022-22526-7
74. Jayamani T, Arul Prasad A, Edal Queen TJ, Scholastica Mary Vithiya B, Tamizhdurai P, Siva Kumar N, Al-Fatesh AS, Reddy J, Koduru (2023) Catalytic reduction of anionic and cationic toxic dyes and evaluation of antimicrobial activity using green synthesized palladium nanoparticles employing Carica papaya aqueous leaf extract. J Saudi Chem Soc 27:101759. https://doi.org/10.1016/j.jscs.2023.101759